Soft particle production in deep inelastic scattering

Nick Brook †
on behalf of the H1 and ZEUS Collaborations

H H Wills Physics Laboratory, University of Bristol, Tyndall Avenue, Bristol BS8 1TL, UK.

E-mail: n.brook@bristol.ac.uk

Abstract. Results on the analysis of the hadronic final state in neutral current deep inelastic scattering at HERA are presented; recent results on inclusive single particle distributions, particle correlations and event shapes are highlighted.

1. DIS kinematics

The event kinematics of deep inelastic scattering, DIS, are determined by the negative square of the four-momentum transfer at the lepton vertex, $Q^2 \equiv -q^2$, and the Bjorken scaling variable, $x = Q^2/2P \cdot q$, where P is the four-momentum of the proton. In the quark parton model (QPM), the interacting quark from the proton carries the four-momentum xP. The variable y, the fraction of the energy transferred to the proton in the proton rest frame, is related to x and Q^2 by $y \simeq Q^2/xs$, where $\sqrt{s}$ is the positron-proton centre of mass energy. Neutral current (NC) DIS occurs when an uncharged boson (γ, Z^0) is exchanged between the lepton and proton.

A natural frame in which to study the dynamics of the hadronic final state in DIS is the Breit frame [1]. In this frame, the exchanged virtual boson (γ^*) is completely space-like and has a four-momentum $q = (0, 0, 0, -Q = -2xP^{Breit}) \equiv (E,\ p_x,\ p_y,\ p_z)$, where P^{Breit} is the momentum of the proton in the Breit frame. The particles produced in the interaction can be assigned to one of two regions: the current region if their z-momentum in the Breit frame is negative, and the target region if their z-momentum is positive. The main advantage of this frame is that it gives a maximal separation between the incoming and outgoing partons in the QPM. In this model the maximum momentum a particle can have in the current region is $Q/2$, while in the target region the maximum is $\approx Q(1 - x)/2x$. In the Breit frame, unlike the hadronic centre-of-mass $(\gamma^* p)$ frame, the two regions are asymmetric, particularly at low x, where the target region occupies most of the available phase space.

† PPARC Advanced Fellow

2. Current fragmentation region

The current region in the Breit frame of DIS is analogous to a single hemisphere of e^+e^- annihilation. In this region, the outgoing struck quark from the proton has a momentum $-Q/2$. The scaled momentum spectra of the particles in the current region, expressed in terms of $\xi_p = \ln(Q/2p^{Breit}) = \ln(1/x_p)$, are expected to have a dependence on Q similar to that observed in e^+e^- annihilation [2] at energy $\sqrt{s_{ee}} = Q$. It is convenient to investigate these spectra in terms of moments.

One approach that has been successful in describing the general features of the inclusive energy spectra, in both e^+e^- annihilation and deep inelastic scattering (DIS) experiments [2, 3], is the modified leading log approximation (MLLA). This uses the local parton hadron duality (LPHD) approach [4] to relate the MLLA partonic predictions to the hadronic observables. These MLLA calculations have two free parameters: a running strong coupling, defined by a QCD scale Λ, and an energy cut-off, Q_0, below which the parton evolution is truncated. The so-called limiting spectrum [4] is the case when $Q_0 = \Lambda$. LPHD assumes that a simple normalisation factor can be used to relate the hadronic to the partonic distributions. At large enough energies, away from where the parton evolution is truncated, this 'hadronisation' factor should be approximately independent of the energy scale [4] at which the parton spectra are calculated.

The analytic form of the cumulant moments, within the framework of MLLA and LPHD, has been calculated [5] for the first four moments. This allows the normalised moment, $\langle \xi^m \rangle$, to be calculated and hence the width (σ), skewness (s) and kurtosis (k) to be constructed [6].

In the MLLA approach discussed above, the partons are assumed massless so the scaled energy and momentum spectra are identical. Experimentally the scaled momentum distribution is usually measured and as the observed hadrons are massive the equivalence of the two spectra no longer holds. It can be assumed [7, 8] that the cut-off Q_0 can be related to an effective mass, $m_{\rm eff}$, of the hadrons. This allows the logarithmic scaled momentum distribution, ξ_p, to be related to the scaled energy distribution. The limiting momentum spectra based on massless partons or massive partons with $m_{\rm eff}$ being set to $Q_0 \equiv \Lambda$, will be referred to as MLLA-0 and MLLA-M spectra, respectively. This effective mass does not have to be fixed to Λ but can be treated as an additional free parameter of the theoretical models and can be fitted to the data.

The moments of the ξ_p distributions have been investigated up to the 4th order [9]; the mean (l), width (σ,) skewness (s) and kurtosis (k) were extracted from each distribution by fitting a distorted Gaussian of the following form:

$$\exp\left[\frac{1}{8}k - \frac{1}{2}s\delta - \frac{1}{4}(2+k)\delta^2 + \frac{1}{6}s\delta^3 + \frac{1}{24}k\delta^4\right]$$

where $\delta = (\xi - l)/\sigma$. The equation is motivated by the expression used for the MLLA predictions of the spectra [10].

To study the differences between the MLLA predictions and the data, fits of a distorted Gaussian have been made to the MLLA predictions, in a manner similar to

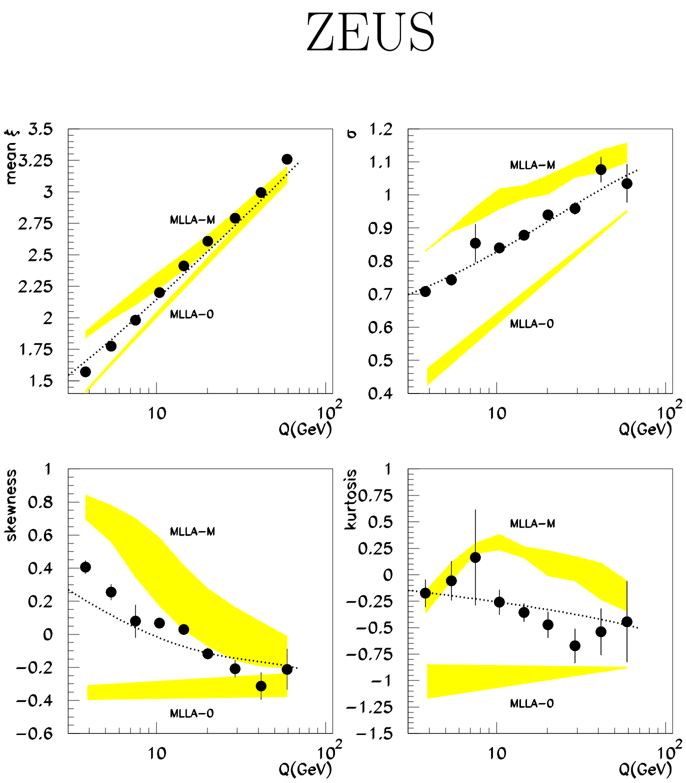

Figure 1. The moments of the ξ_p distribution in the current fragmentation region as a function of Q, from fits to ZEUS data, are shown as solid points. The errors are those returned from the fit. The upper and lower shaded areas are from fits to the MLLA-M and MLLA-0 spectra, respectively. The dotted line shows the moments obtained from a fit to the MLLA spectrum obtained using the fitted $\Lambda = 280$ MeV, $m_{\text{eff}} = 230$ MeV.

the fits made to the data, in order to extract the moments [8]. Figure 1 shows the first four moments of the ξ_p spectra as a function of Q. For the ZEUS data, the mean and σ increase as Q increases, whilst the skewness and kurtosis fall. For both MLLA-M and MLLA-0, the range fitted lay between 30% of the spectrum (lower limit of band) to 80% of the spectrum as measured from the maximum of the differential distributions.

For σ, skewness and kurtosis, Fig. 1, the DIS data lie in between the MLLA-M and MLLA-0 predictions. The skewness predicted by MLLA-M is more positive than the data while MLLA-0 underestimates the skewness; for the highest Q, both models approach the data. There is evidence of a systematic difference in the Q-dependence of the mean between the models and the data for the energy range studied here.

Also shown are the moments obtained from a fit to the massive MLLA spectrum obtained using the fitted $\Lambda = 280$ MeV and $m_{\text{eff}} = 230$ MeV. It is evident that a reasonable description of all moments other than the mean is obtained; the mean has an energy dependence that differs from that of the data.

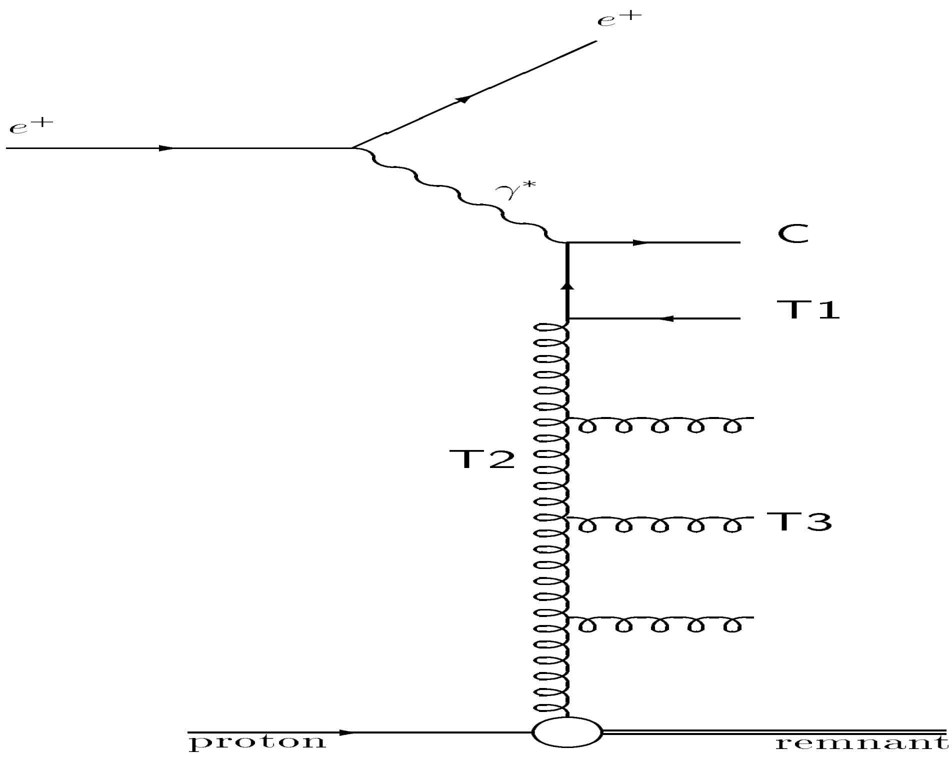

Figure 2. A schematic of DIS scattering at low x within the MLLA framework. Quark C represents the struck sea quark in the current fragmentation region. T1 is the other half of the quark box which is in the target region. T2 is the t-channel gluon exchange and T3 the rungs of the gluon ladder.

3. Target fragmentation

DIS at low x allows a study of fragmentation in the target region following the initial scattering off a sea quark (or antiquark). The description based on MLLA [2] is shown schematically in Fig. 2, where the quark box at the top of the gluon ladder represents the scattered sea quark plus its antiquark partner. There are various contributions to these calculations. Contribution C, the top leg of the quark box, corresponds to fragmentation of the outgoing quark in the current region. Three further contributions (T1, T2 and T3), which are sources of soft gluons, are considered in these analytic calculations to be associated with the target region. It is predicted [2] that the contribution T1 (the bottom leg of the quark box) behaves in the same way as the current quark C and so should have no x dependence. The contribution T2 is due to the colour field between the remnant and the struck quark, and the contribution T3 corresponds to the fragmentation of the rungs in the gluon ladder. Both T2 and T3 are predicted to have x and Q^2 dependences which differ from T1. Both the T1 and T2 contributions have been calculated and give particles of momenta $< Q/2$. The collinear gluons T3, on the other hand, generally fragment to particles with momentum $\gtrsim Q/2$. For values of the scaled momentum $x_p < 1.0$, the region of phase space is analogous to the current region and has contributions mainly from T1 and T2. The parton momentum spectra predicted by MLLA, over a range of Q^2 and x, are shown in more detail elsewhere [11]. In the target region these spectra are approximately Gaussian for $x_p < 1$; they peak at a value of $x_p \sim 0.1 - 0.2$ in the range of x and Q^2 measured by ZEUS [9], falling to a plateau region for $1 < x_p < (1-x)/x$ (the maximum value of x_p in the target region).

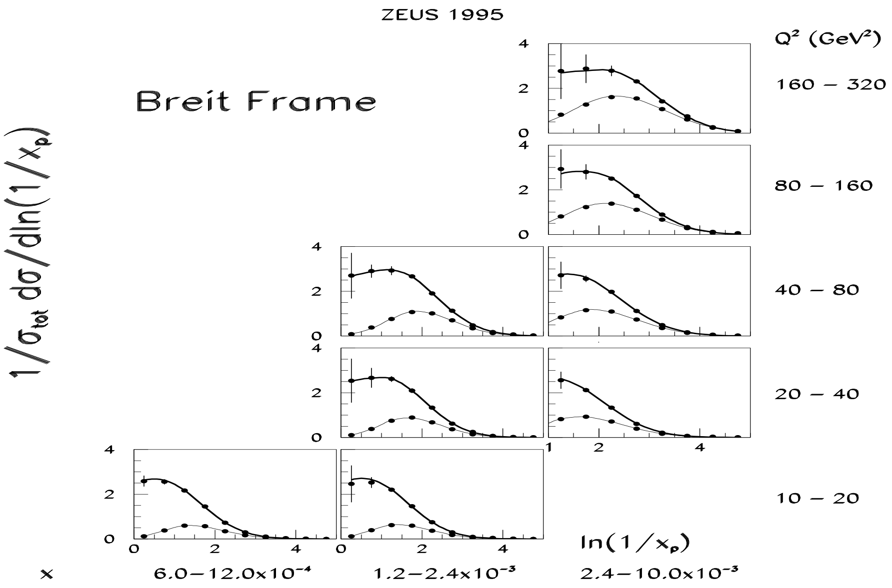

Figure 3. The corrected $\ln(1/x_p)$ distributions for the target and current regions for the 1995 data. Fitted two-piece normal distributions are shown to guide the eye. The heavy line corresponds to the target region, the light line to the current region. The error bars are the sum of the statistical and systematic errors in quadrature.

The distributions in $\ln(1/x_p)$ are shown for both the target and current regions in Fig. 3. The fitted curves shown are two-piece normal distributions [12] to guide the eye. In contrast to the current region, the target region distribution does not fall to zero as $\ln(1/x_p)$ tends to zero. Although the magnitude of the single particle density at the peak position of the current region distribution grows by a factor of about three over the Q^2 range shown, the single particle density of the target distribution, at the x_p value corresponding to the peak of the current distribution (contribution C is equivalent to contribution T1), depends less strongly on Q^2 and increases by only about 30%. In addition, the $\ln(1/x_p)$ distribution shows no significant dependence on x when Q^2 is kept constant. In the target region, the peak position of the $\ln(1/x_p)$ distribution increases more rapidly with Q^2 than in the current region; this is consistent with the behaviour expected from cylindrical phase space. The approximate Gaussian distribution of the MLLA predictions peaking at $\ln(1/x_p) \sim 1.5{-}2.5$ [11] is not observed. The results strongly suggest that the target distributions are inconsistent with the MLLA predictions when used in conjunction with LPHD.

4. Multiplicity moments

Multiplicity distributions and correlations between final-state particles are an important testing ground for analytic perturbative QCD (pQCD) in conjunction with the LPHD hypothesis. ZEUS has studied particle multiplicities in terms of the normalised factorial moments

$$F_q(\Omega) = \langle n(n-1)\dots(n-q+1)\rangle / \langle n\rangle^q, \qquad q = 2, 3, \dots,$$

for a specified phase-space region of size Ω. The number, n, of particles is measured inside Ω and angled brackets $\langle\dots\rangle$ denote the average over all events. The factorial moments are convenient tools to characterise the multiplicity distributions when Ω becomes small. For uncorrelated particle production within Ω, Poisson statistics holds and $F_q = 1$ for all q. Correlations between particles lead to a broadening of the multiplicity distribution and to dynamical fluctuations. In this case, the normalised factorial moments increase with decreasing Ω. If the rise follows a power law, this effect is frequently called "intermittency" [13].

The dominant source of particle production inside a jet is gluon splitting in the QCD cascade, where the presence of a gluon enhances the probability for emission of another gluon nearby in momentum space. This leads to inter-parton correlations and non-Poissonian statistics for the multiplicity distributions in restricted phase-space intervals where partons are counted. Thus the factorial moments, F_q, are expected to deviate from unity. There exist a number of analytic QCD predictions for the moments of the parton multiplicity distributions obtained in the Double Leading Log Approximation (DLLA) [14, 15, 16, 17].

The Bose-Einstein (BE) interference between identical particles can produce additional correlations which distort the behaviour of the moments measured in small phase-space regions. To correct the data for this additional effect, the JETSET Monte Carlo (MC) program [18] was used with a Gaussian parameterisation (with the default parameters.) As a cross check, the BE correction was determined from the ZEUS data and also using the parameters obtained by the H1 Collaboration [19]. The differences between the correction factors BE_q for these three sets of parameters were small.

The moments in the current region of the Breit frame were measured [20] in the kinematic region $Q^2 > 1000$ GeV^2. The normalised factorial moments of the multiplicity distributions are restricted in transverse momentum in the Breit frame, $p_t < p_t^{\mathrm{cut}}$. The multiplicity moments of order $q = 2, \dots, 5$ as a function of p_t^{cut} are shown in Fig. 4. As p_t^{cut} decreases below 1 GeV, the moments rise. This disagrees with the DLLA theoretical calculations, which predict that the moments approach unity [14]. On the other hand, Monte Carlo models show the same trend as the data, although some differences in slopes are apparent. LEPTO [21] exhibits smaller values of the moments than for the data at small p_t^{cut} values, while HERWIG [22] overestimates the moments. ARIADNE [23] gives the best overall description of the correlations.

Figure 4 also shows the factors BE_q used to correct the data for the BE interference. The largest correction was found in the case of moments of high orders ($q = 4, 5$) for

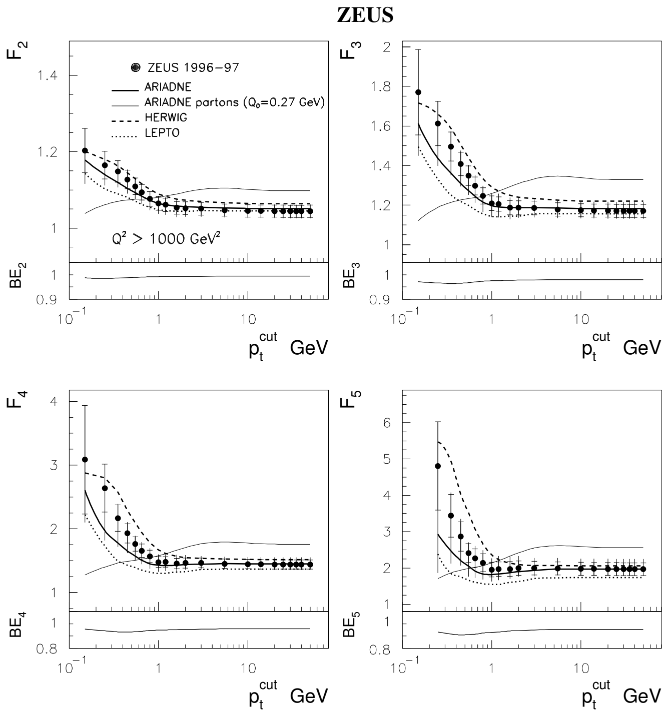

Figure 4. Factorial moments for charged particles in the current region of the Breit frame as a function of $p_t^{\rm cut}$, compared to MC models. The thin lines show the parton-level prediction of ARIADNE with $Q_0 = 0.27$ GeV and the thick solid lines are the hadron-level predictions of the same model. The dashed and dotted lines show the hadron-level predictions of HERWIG and LEPTO, respectively. The inner error bars are statistical uncertainties; the outer are statistical and systematic uncertainties added in quadrature. The correction factors for the BE effect are shown below each plot.

small $p_t^{\rm cut}$ cuts (< 0.5 GeV).

The moments restricted in p_t were determined from the ARIADNE parton-level, the physics implementation of which strongly resembles the analytic calculations [14]. The analytic calculation requires Q_0 to approach Λ. The parton predictions were obtained after switching off the fragmentation and lowering the Q_0 value in ARIADNE to $Q_0 = 0.27$ GeV, which is close to the value of Λ used. This value was chosen in order that the average multiplicity of partons in the current region of the Breit frame equalled that of hadrons, which is important for normalisation purposes.

The parton-level ARIADNE for the moments is shown as thin solid lines in Fig. 4. The parton-level predictions and the data for the lowest $p_t^{\rm cut}$ values are inconsistent. The MC predictions for partons have the trends expected from the analytic DLLA results, showing a decrease of the moments for decreasing $p_t^{\rm cut}$. This is contrary both to the measurements and to the hadron-level MC predictions, which show a rise of the moments.

Gluon multiplicities in polar-angle rings around the outgoing-quark direction are expected to exhibit a distribution which is substantially wider than for Poisson statistics

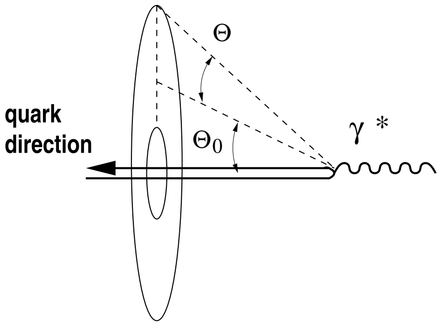

Figure 5. A schematic representation of the measurements of the factorial moments in DIS in polar-angle rings of width 2Θ.

[15, 16, 17]. The moments rise with increasing values of the phase-space variable z as

$$\ln \frac{F_q(z)}{F_q(0)} = z\, a\,(1 - D_q)(q - 1),$$

where z and the constant a are defined as:

$$z = a^{-1} \ln \frac{\Theta_0}{\Theta} \quad \text{and} \quad a = \ln \frac{E\Theta_0}{\Lambda}.$$

The angle Θ_0 is the half opening-angle of a cone around the outgoing quark radiating the gluons, E is its energy, and Λ is an effective QCD scale. A schematic representation of the variables is shown in Fig. 5, in which a window in the angular half-width Θ is subtended by the ring centered at Θ_0. The factors D_q are the so-called Rényi dimensions [24] known from non-linear physics. A decrease of the angular window Θ corresponds to an increase of the variable z. The maximum possible phase-space region ($\Theta = \Theta_0$), corresponding to $z = 0$, is used to calculate the factorial moments, $F_q(0)$, which are necessary for normalisation. Such normalisation removes the theoretical uncertainty in the absolute values of $F_q(z)$ and thus allows a comparison of the predicted z-dependence of the moments with experimental results.

For independent particle production in a restricted range of 2Θ, $D_q = 1$ and $F_q(z) = F_q(0)$. In contrast, the analytic QCD expectations for D_q obtained in the DLLA [15, 16, 17] without and with running α_s and different assumptions on the non-leading terms lead to values of D_q that are non-unity. A prediction within the MLLA framework also exists [15].

Figure 6 shows the angular moments $F_q(z)/F_q(0)$. The measurements [20] are compared to DLLA QCD calculations, using the effective QCD parameter $\Lambda = 0.15$ GeV as in LEP studies [25]. For DIS in the Breit frame, the energy $E = Q/2$ was chosen to define the α_s value, corresponding to the outgoing quark momentum in the quark-parton model. The factors used to correct the data for the BE interference are close to unity for all angular moments (not shown). A significant disagreement with the

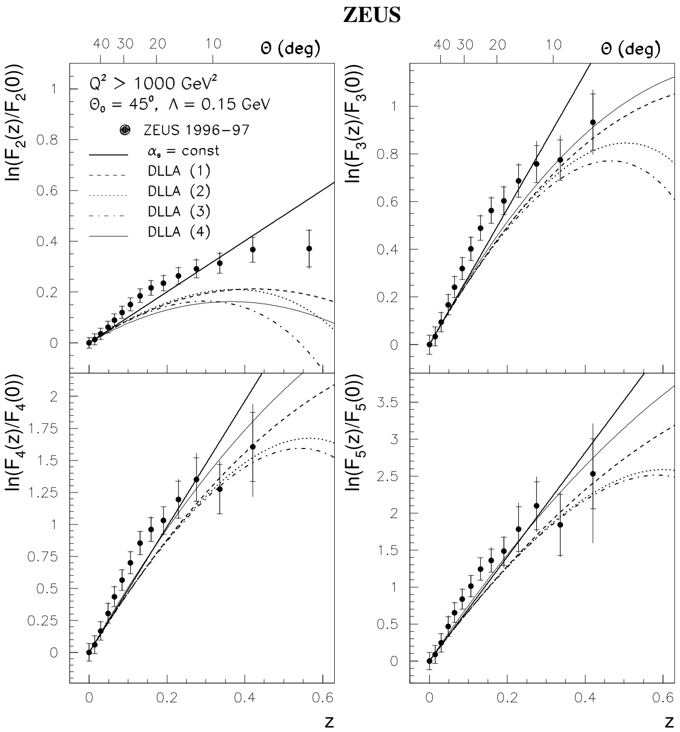

Figure 6. $F_q(z)/F_q(0)$ ($q = 2, \ldots, 5$) as a function of the scaling variable z for $\Theta_0 = 45^o$ and $\Lambda = 0.15$ GeV, compared to the QCD predictions with different parameterisations of D_q: $\alpha_s =$ const (bold solid lines); (1) DLLA of ref. [15](dashed lines); (2) DLLA of ref. [16] (dotted lines); (3) DLLA of ref. [17] (dash-dotted lines); and (4) DLLA with a correction from the MLLA [15] (thin solid lines). The values of Θ are given at the top of the plots. The inner error bars are statistical uncertainties; the outer are statistical and systematic uncertainties added in quadrature.

data is observed, which becomes smaller for higher orders of the moments. Although the error bars are clearly correlated, even for the high-order moments, agreement between the predictions and the data can be excluded. For running-α_s calculations, the best description is observed for high-order moments in the case of the DLLA result with a correction from the MLLA. This result is similar to those obtained for e^+e^- annihilation [25]. It should be noted that the present analysis, however, uses a larger angle $\Theta_0 = 45^o$, in order to increase the statistics, and that the average energy ($\langle E \rangle \simeq 23$ GeV) of the outgoing quark giving rise to the parton shower is smaller than at LEP by a factor of two.

5. Event shapes

The event shape dependence on Q can be due to the logarithmic change of the strong coupling constant $\alpha_s(Q) \propto 1/\ln Q$, and/or power corrections (hadronisation effects) which are expected to behave like $1/Q$. Recent theoretical developments suggest that $1/Q$ corrections are not necessarily related to hadronisation, but may instead be a universal soft gluon phenomenon associated with the behaviour of the running coupling at small momentum scales [26]. These non-perturbative corrections are governed by a parameter $\bar{\alpha}_0$. The scale dependence of any event shape mean $\langle F\rangle$ can be written as the sum of two terms: one associated with the perturbative contribution, $\langle F\rangle^{\mathrm{pert}}$, and the other related to the power corrections, $\langle F\rangle^{\mathrm{pow}}$. The perturbative contribution to an event shape can be calculated from NLO programs, such as DISENT [27].

In the power correction approach [26] $\langle F\rangle^{\mathrm{pow}}$ is parameterised as follows:

$$\langle F\rangle^{\mathrm{pow}} = a_F \frac{32}{3\pi^2}\mathcal{M}\left(\frac{\mu_I}{Q}\right) \left[\bar{\alpha}_0(\mu_I) - \alpha_s(Q) - \frac{\beta_0}{2\pi}\left(\ln\frac{Q}{\mu_I} + \frac{K}{\beta_0} + 1\right)\alpha_s^2(Q)\right],$$

where β_0 and K are constants dependent on the number of flavours, a_F is a calculable coefficient dependent on the observable F, μ_I is an 'infrared' matching scale (μ_I = 2 GeV), $\frac{2}{\pi}\mathcal{M} \approx 0.95$ is a 2-loop correction and $\bar{\alpha}_0$ is a universal, non-perturbative effective strong coupling below μ_I.

At HERA, a number of infrared-safe event-shape variables have been investigated [28, 29] in the range $7 < Q < 140$ GeV. Event-shapes studied in the current region are: thrust, with respect to the Breit axis τ (or τ_z) and the thrust axis τ_c (or τ_m), jet broadening B with respect to the Breit frame axis, the C parameter and jet mass ρ and ρ_0. Also investigated was the variable y_{fJ} (over the whole of phase space). This variable represents the transition value for $(2+1) \to (1+1)$ jets of the factorizable JADE algorithm for a particular event.

A common feature of all the mean event-shape values, illustrated in Fig. 7, is the fact that they exhibit a decrease with rising Q. This is due to the fact that the energy flow becomes more collimated along the event-shape axis as Q increases, a phenomenon also observed in e^+e^- annihilation experiments. ZEUS has binned in both x and Q and in some regions has measured the event shapes in the same range in Q but different x ranges. The data, particularly B, exhibit a stronger dependence on x than that predicted from the NLO calculations. In general, power corrections have no dependence on x; however, such terms may arise for B [30]. The fits to the data are also shown.

The results of the fit are shown in Fig. 8; H1 and ZEUS are consistent. The parameter $\bar{\alpha}_0$ is observed to be ≈ 0.5 for all event shapes (except for the jet rate parameter y_{fJ}, not shown), consistent with theoretical expectation. However, there is a large spread in the values of α_s.

The treatment of hadron masses has a considerable impact on the jet mass variable, which is calculated from particle four-momenta. Fitting power corrections to the energy dependence of the mean jet mass while assuming massless hadrons, ρ_0, reduces the spread of the non-perturbative parameter $\bar{\alpha}_0$ and of the strong coupling, α_s.

The theoretically calculated parameter for the power corrections for y_{fJ} was $a_{y_{fJ}} = 1$. This is contrary to the observed need for small negative hadronisation corrections [28]. A reasonable fit for y_{fJ} was achieved by using a value of $a_{y_{fJ}} = -0.25$.

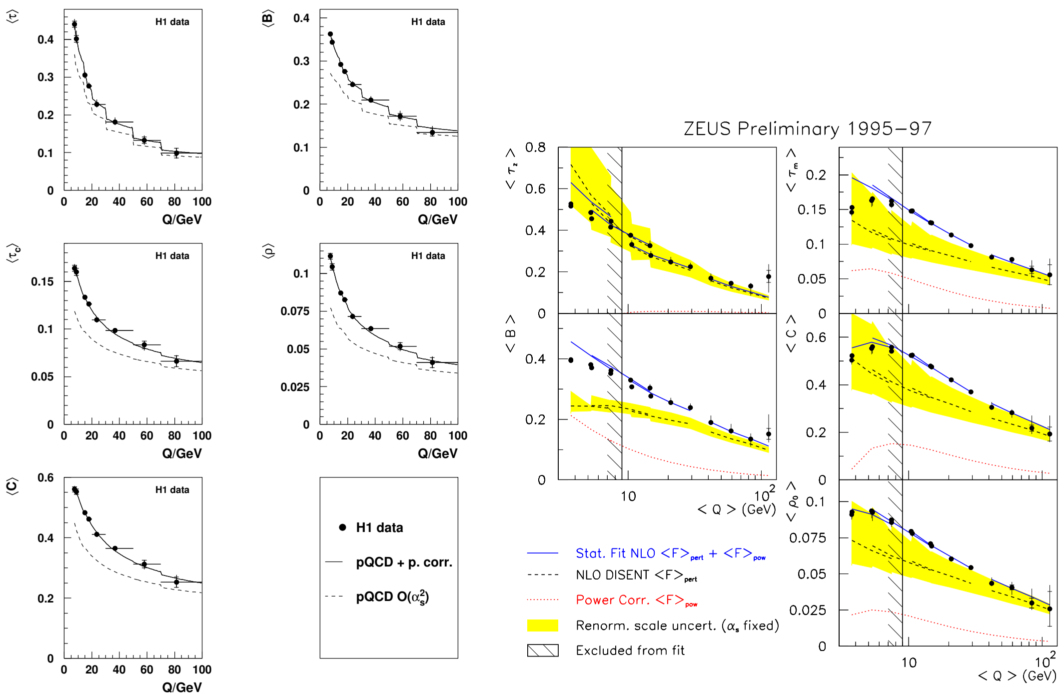

Figure 7. The points are the corrected mean values of various event shapes variables as a function of Q for H1 and ZEUS. The inner error bars on the data show the statistical uncertainties. The full error bars include the systematic uncertainties. The full line corresponds to a power correction fit according to the approach in [26]. The dashed line is the perturbative (NLO) prediction from DISENT using the value of α_s found from the full fit.

The basic concept of approximate universal power corrections is generally supported by the HERA experiments. However, there remain several open questions. The data require further theoretical progress concerning the jet rates and x-dependence of power corrections and resummed QCD calculations.

6. Summary

To understand the underlying QCD processes in DIS, it is necessary to study the hadronic final state. At the current level of understanding, QCD works well and describes the HERA data. As the precision of the HERA data improves and further NLO QCD calculations become available, the framework of QCD is being tested more thoroughly.

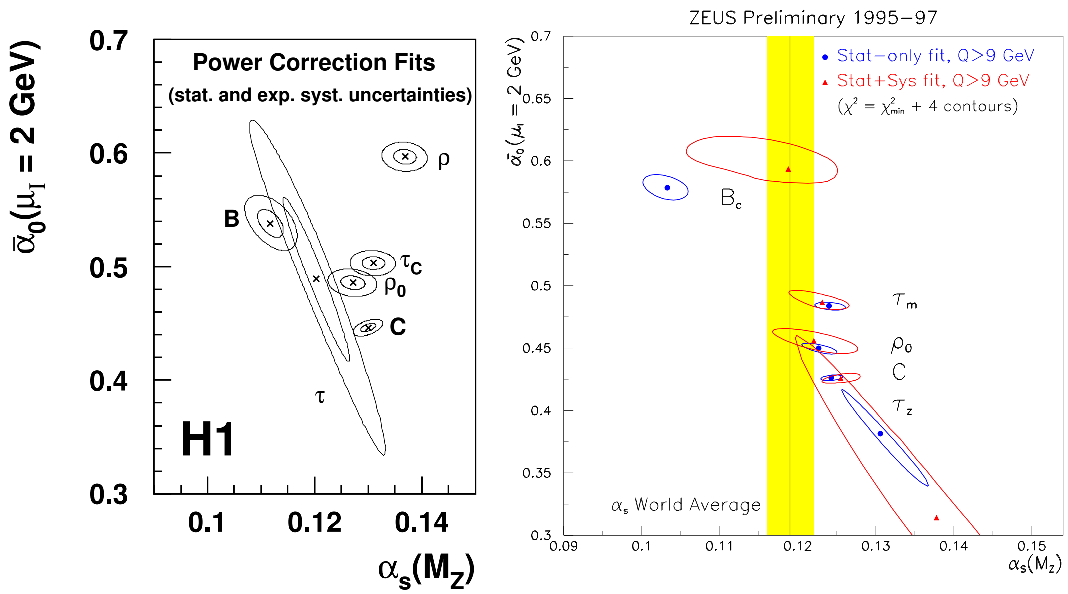

Figure 8. Results of the fit to $\bar{\alpha}_0$ and α_s for the means of the event shape variables. The H1 results show the $\chi^2 = \chi^2_{\rm min} + 1$ and $\chi^2 = \chi^2_{\rm min} + 4$ contours for statistical and experimental systematic errors combined in quadrature. The smaller contours in the ZEUS results are a statistical only fit, the larger ones are the $\chi^2 = \chi^2_{\rm min} + 4$ contours for the statistical and systematic errors combined in quadrature.

References

[1] Feynman R P 1972 *Photon-Hadron Interactions* (New York, Benjamin).

[2] Dokshitzer Yu *et al* 1988 *Sov Phys JETP* **68** 1303.

[3] Khoze V A and Ochs W 1997 *Int. J. Mod. Phys.* A**12** 2949.

[4] Azimov Ya I *et al* 1985 *Z. Phys.* C**27** 65; Azimov, Ya I *et al* 1986 *Z. Phys.* C**31** 213.

[5] Dokshitzer Yu, Khoze V A and Troyan S 1972 *Int. J. Mod. Phys.* A**7** 1875.

[6] Stuart A and Ord J K 1987 *Kendall's Advanced Theory of Statistics* (London, Griffin).

[7] Khoze V A, Lupia S and Ochs, W 1996 *Phys. Lett.* B**386** 451.

[8] Brook N H and Skillicorn I O 2000 *Phys. Lett.* B**479** 173; Brook N H and Skillicorn I O 2001 *Phys. Lett.* B**497** 55.

[9] ZEUS Collaboration, Breitweg J *et al* 1999 *Eur. J. Phys.* C**11** 251.

[10] Fong C P and Webber B R 1989 *Phys. Lett.* B*229* 289; Fong C P and Webber B R (1991) *Nucl. Phys.* B**355** 54.

[11] Anisovich A V 1993 Il Nuovo Cimento A**106** 547.

[12] Bank of England Quarterly Bulletin February 1998 and references therein.

[13] Białas A and Peschanski R 1986 *Nucl. Phys.* B**273** 703; Białas A and Peschanski R 1988 *Nucl. Phys.* B**308** 857.

[14] Lupia S, Ochs W and Wosiek J 1999 *Nucl. Phys.* B**540** 405.

[15] Dokshitzer Yu and Dremin I M 1993 *Nucl. Phys.* B**402** 139.

[16] Brax P, Meunier J-L and Peschanski R 1994 *Z. Phys.* C**62** 649.

[17] Ochs W and Wosiek J 1992 *Phys. Lett.* B**289** 159; Ochs W and Wosiek J 1993 *Phys. Lett.* B**305** 144; Ochs W and Wosiek J 1995 *Z. Phys.* C**68** 269.

[18] PYTHIA 5.7 and JETSET 7.4, Sjöstrand T 1994 Comp. Phys. Comm. **82** 74.

[19] H1 Collaboration, Adloff C *et al* 1997 *Z. Phys.* C**75** 437.

[20] ZEUS Collaboration, Chekanov S *et al* 2001 *Phys. Lett.* B**510** 36.

[21] LEPTO 6.5, Ingelman G, Edin A and Rathsman J 1997 Comp. Phys. Comm. **101** 108.
[22] HERWIG 5.1, Marchesini G *et al* 1992 Comp. Phys. Comm. **67** 465.
[23] ARIADNE 4.10, Lönnblad L 1992 Comp. Phys. Comm. **71** 15; Lönnblad L 1999 *Proceedings of the 1998/1999 Workshop on Monte Carlo Generators for HERA Physics (Hamburg)* (Hamburg: DESY) p 47.
[24] Rényi A 1970 *Probability Theory* (Amsterdam, North-Holland); Hentschel H G E and Procaccia I 1983 Physica D**8** 435; Grassberger P 1983 *Phys. Lett.* A**97** 227.
[25] L3 Collaboration, Acciarri M *et al* 1998 *Phys. Lett.* B**428** 186; L3 Collaboration, Acciarri M *et al* 1998 *Phys. Lett.* B**429** 475; DELPHI Collaboration, Abreu P *et al* 1999 *Phys. Lett.* B**457** 368.
[26] Dokshitzer Yu and Webber B R 1995 *Phys. Lett.* B**352** 451; Webber B R 1995 *Proc. DIS'95, 5th International workshop on Deep Inelastic Scattering (Paris)* (Paris: Ecole Polytechnique) p 115.
[27] Catani S and Seymour M H 1997 *Nucl. Phys.* B**485** 291; erratum- Catani S and Seymour M H 1997 *Nucl. Phys.* B**510** 503.
[28] H1 Collaboration, Adloff C *et al* 2000 Eur. Phys. J. C**14** 255; addendum - H1 Collaboration, Adloff C *et al* 2000 Eur. Phys. J. C**18** 417.
[29] ZEUS Collaboration, paper 421 to ICHEP 2000.
[30] Dasgupta M 2001 Private communication.